Electronic Journal of Structural Engineering

Original Article

Cite this: DOI:10.56748/ejse.24499

Received Date:30 July 2023
Accepted Date:14 January 2024

1443-9255
https://ejsei.com/ejse

Research on evolution characteristics of multi-information and stability for deep tunnel underlaying goaf

Feiyue Sun[a, c], Jiaqi Guo[b, c], Xiaobing Zhang[a *], Shaohua Li[d], Xiliang Liu[b, c]
[a] School of Emergency Management, Henan Polytechnic University, Jiaozuo 454003, Henan, China
[b] School of Civil Engineering, Henan Polytechnic University, Jiaozuo 454003, Henan, China
[c] Key Laboratory of Henan Province for Underground Engineering and Disaster Prevention, Jiaozuo 454003, Henan, China
[d] China Railway 15th Bureau Group Co., Ltd., Shanghai 200000, China
*Corresponding author: xiaobingzhang@hpu.edu.cn

Abstract

To ensure the safety of construction and operation of the tunnel near the goaf. Based on dynamic numerical analysis, three-dimensional finite difference numerical simulation software was developed by FISH programming. Then, on basis of the construction of practical engineering, the safety distance and energy evolution mechanism in an underlying mining goaf area of deep tunnel are studied. The results show that according to the different safe distance in an underlying mining goaf area of deep tunnel, the tunnel structure is divided into danger zone, influence zone and safe zone. The relationship between the cumulative horizontal energy and stress ratio can be divided into three stages: acceleration, average stability, and deceleration. The energy evolution of the three stages can also better reflect the damage and failure mechanism inside the surrounding rock mass. The measured field curve shows that when the safety distance is 12 m, the goaf has limited influence on the stability of the tunnel, and the construction in an underlying mining goaf area of deep tunnel is stable overall and meets the safety requirements. The best safe distance between the tunnel and goaf is about one time of the tunnel span.

Keywords

deep tunnel, goaf, safety distance, stability evaluation, numerical simulation

1. Introduction

With the rapid development of tunnel construction in China, bad geological sections of goaf are often encountered inevitably in tunnel engineering through mountainous areas. When the tunnel crosses the goaf, the settlement deformation of the goaf may lead to uneven settlement of the tunnel above. And then caused traffic accidents, resulting in tunnel structure deformation, cracking, tunnel construction and later operation to bring serious safety risks (Chu et al. 2020; Wang et al. 2020). Therefore, reasonable determination of the safety distance between the tunnel and the underlying goaf, as well as the evaluation of the safety stability of the underlying goaf, has become an urgent technical problem to be solved when building the tunnel project above the goaf.

The safety and stability problems faced by the construction of tunnels in the goaf area have attracted the attention of scientific researchers and engineering researchers, and a lot of research has been carried out. In experimental study, Ram et al. (2021) proposed a novel design of rock bolts as goaf edge support. Zheng et al. (2021) studied the coupling evolution of air and temperature field in coal mine goafs. Wang et al. (2022) proposed a theoretical method to calculate the goaf resistance of ventilation air leakage pathways. Liu et al. (2023) established the constitutive relation and particle size distribution model of rock fragments in the goaf. Xu et al. (2023) investigated the monitoring and stability evaluation of ground subsidence in gypsum mine goaf. Zhang et al. (2023) obtained the optimal backfill parameters for the goaf treatment by a series of mechanical tests. Wang et al. (2024) established the multi-parameter fusion goaf fire early warning index system based on the D-S evidence theory of weight allocation. With the rapid development of computer technology, numerical simulation has become a mainstream method for geotechnical engineering research and design. Zhang et al. (2019) investigated the mechanical property of constructing tunnel underlying inclined goaf. Cui et al. (2019) analyzed the construction safety and stability during the construction of a typical deep-buried tunnel crossing complex goaf. Zhang et al. (2021) proposed a novel 3D simulation method for broken rock mass in goaf. Islavath et al. (2022) established that once longwall face approaches near the fault zone, goaf formation must be avoided to improve the stability at the face. Vinay et al. (2022) studied the effect of goaf on pillar stability. Zhao et al. (2023) investigated the effects of the friction coefficient of the pipe and soil, the coal-seam dip angle, and the horizontal angle on the mechanical behavior of the pipe under varying widths of goaf area. Fu et al. (2024) analyzed the formation conditions, judgment principles, and judgment methods of the dangerous area of gas explosion coupling disaster in goaf.

The above research results mainly focus on the research of the unstable collapse of the goaf on the mechanical behavior of tunnel construction, the mechanism of deformation instability and the stability of the surrounding rock mass. However, when the tunnel passes through the unfavorable geological section of the goaf, the safe distance between the tunnel and the goaf is a key factor affecting the stability of the tunnel and the safety of construction and operation, and to a certain extent determines the design requirements such as tunnel alignment and buried depth. To further ensure the safety of tunnel construction in goaf section and minimize the influence of goaf on tunnel construction, it is necessary to study the safety distance and stability of goaf under deep tunnel. In view of this, based on the three-dimensional finite difference numerical simulation platform and the actual engineering case, this paper studies the deformation characteristics, stress distribution characteristics, energy evolution mechanism and dynamic response of surrounding rock mass of deep tunnel under different safety distances. Meanwhile, the on-site safety and stability assessment was carried out. The research results have very important engineering application value in this field and can provide reference for similar projects.

2. Numerical calculation of safety distance in construction of goaf under deep tunnel

2.1 Engineering situations

The total length of the right tunnel is about 8168 m, and the maximum buried depth is 611 m, and the total length of the left tunnel is about 8151 m, and the maximum buried depth is 584 m. It is designed according to the standard of two-way four-lane 80 km/h expressway and adopts the separated double-hole layout. There are three goafs at K106+280~+358 on the right line of the tunnel, and the lithology of the tunnel area is mainly mudstone, marl, and sandy mudstone. The stability of the surrounding rock mass in the goaf section is poor, and the tunnel vault is prone to collapse and uneven settlement. The location and layout of the tunnel are shown in Fig. 1 (Lei et al. 2019).

2.2 Establishing the numerical analysis model

Numerical model and boundary conditions

To ensure the authenticity and reliability of the simulation results, according to the Saint Venant principle and the influence range of tunnel excavation and eliminating the boundary effect caused by the simulation calculation. The established calculation model has a transverse length of

100 m, a vertical height of 100 m and a longitudinal width of 60 m. The goaf is simplified as a circular cavity, located on the lower side of the tunnel, with a radius of 3 m and a length of 18 m. The numerical calculation model is shown in Fig. 2.

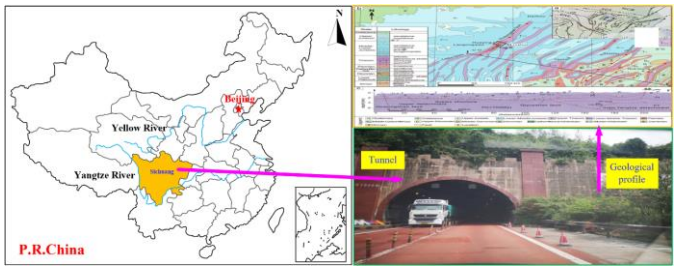

Fig. 1 Location and layout of tunnel

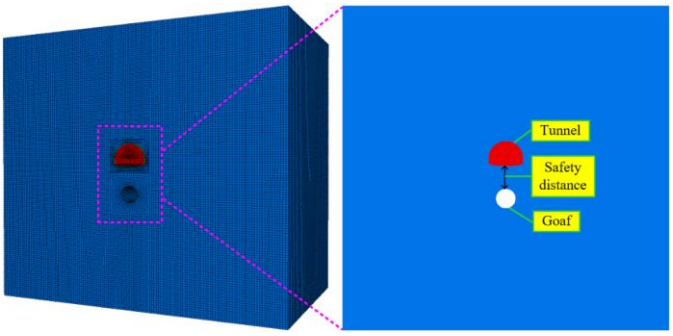

Fig. 2 Three-dimensional model of tunnel

The upper boundary of the model is a stress constrained boundary condition, and the vertical load of 19.62 MPa (field measurement) is applied. The lower boundary, front, and rear boundary left, and right boundary of the model are all displacement constrained boundary conditions. The outer boundary of the model is set as a static boundary to reduce or eliminate the reflection of elastic wave generated by simulation calculation.

Action form of blasting load

Since rock blasting is a complex process generated instantaneously, the explosion mechanism and its influencing factors are extremely complex, it is difficult to quantitatively determine the details of the explosion process. In the numerical analysis, the blasting load is often assumed to be a triangular shock wave (Zhou et al. 2015; He et al. 2017). Through the secondary development of three-dimensional finite difference software, the dynamic load is applied by using FISH programming language, which is applied to the tunnel excavation profile by using APPLE command. In the dynamic calculation, to quickly absorb the kinetic energy of the system to achieve convergence, Rayleigh damping is used for damping, the minimum critical damping ratio is set to 0.25, and the minimum center frequency is set to 550 Hz.

Constitutive model and material mechanics parameters

In the numerical calculation, the constitutive relation of the model adopts Mohr-Coulomb yield criterion (Peng et al. 2020). The physical and mechanical parameters of the material are shown in Table 1. The simulations in this paper make assumptions about the lithology of the rock mass: the rock mass is a homogeneous and isotropic continuum, which conforms to the Mohr-Coulomb strength criterion, and the material parameters satisfy the Mohr-Coulomb constitutive model relationship.

Table 1 Physical and mechanical parameters of the material

Materials	Elasticity modulus (GPa)	Density (kg/m³)	Poisson's ratio	Internal friction angle (°)	Cohesion (MPa)
Surrounding rock mass (IV)	5	2256	0.35	30	0.52
Initial support	25	2500	0.22	—	—
Secondary lining	30	2500	0.20	—	—

2.3 Numerical analysis scheme and monitoring point layout

In the numerical analysis, the safe distances between the tunnel and the goaf are 0.25L, 0.50L, 0.75L, 1L, 1.25L, and 1.50L (L is the tunnel span, rounded to 12 m), as shown in Table 2. The layout of monitoring points is shown in Fig. 3.

Table 2 Numerical experiment scheme

Working condition		1	2	3	4	5	6
Safe distance D		0.25L	0.50L	0.75L	1L	1.25L	1.50L
Actual distance (m)	H	3	6	9	12	15	18

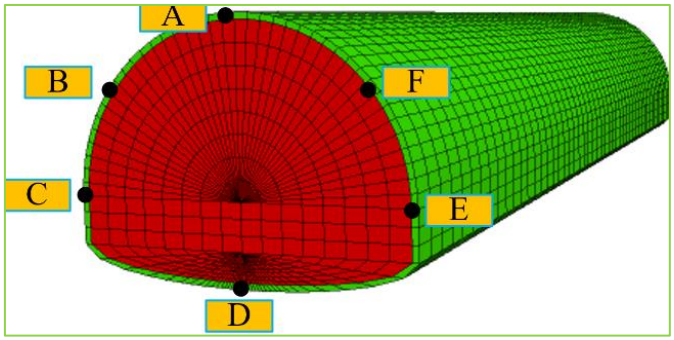

Fig. 3 Monitoring points position

3. Simulation results and analysis

3.1 Evolution process of displacement field in surrounding rock mass

The displacement variation curves of the top-to-floor and the two sides in tunnel for each working condition are shown in Figs. 4-5, respectively. Among them, the deformation of the vault is negative, which represents subsidence, and the deformation of the arch bottom is positive, which represents uplift. The displacement of the left wall of the tunnel is positive, which represents the displacement of the surrounding rock mass to the right side of the tunnel. The displacement of the right wall of the tunnel is negative, which represents the displacement of the surrounding rock mass to the left side of the tunnel.

The contour maps of vertical and horizontal displacement of surrounding rock mass in each working condition are shown in Figs. 6-7 respectively.

(1) The displacement curves of the top-to-floor and the two sides in tunnel show that the deformation of the surrounding rock mass decreases with the increase of the safe distance between the tunnel and the goaf, and the reduction is more obvious. At the top and floor of the tunnel, the deformation of H=18 is reduced by 30.19% and 47.16% respectively compared with H=3. At the left and right-side walls of the tunnel, the displacement curves of the side walls on both sides of the tunnel surrounding rock mass are roughly symmetrically distributed. With the increase of the distance from the center of the tunnel, the displacement deformation of the two sides of the surrounding rock mass gradually decreases, and the closer the distance from the center of the tunnel, the greater the deformation of the surrounding rock mass. It shows that the response of the tunnel entrance to the explosion is the most obvious.

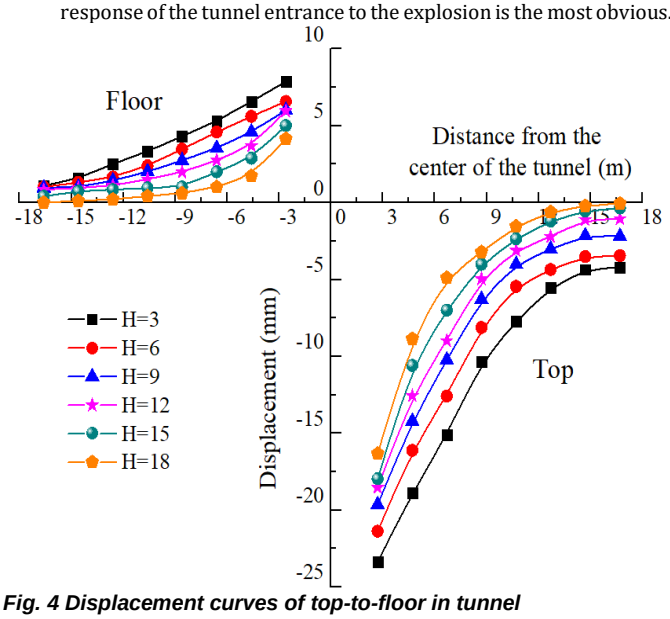

Fig. 4 Displacement curves of top-to-floor in tunnel

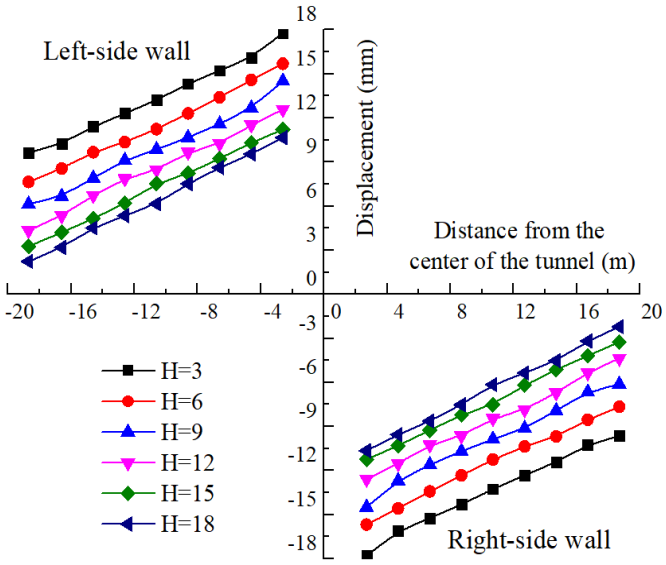

Fig. 5 Displacement curves between two sides of tunnel

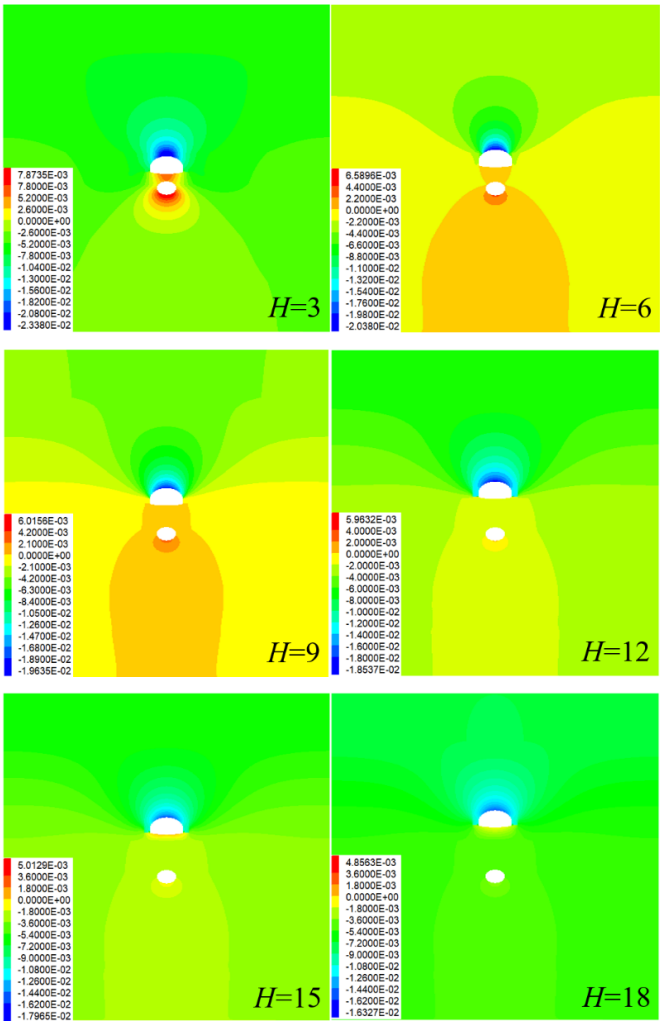

Fig. 6 Contour maps of vertical displacement (unit: m)

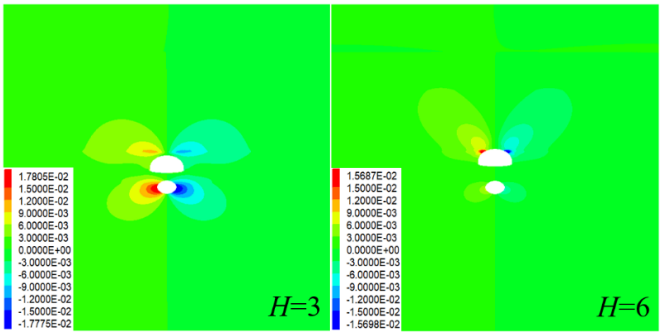

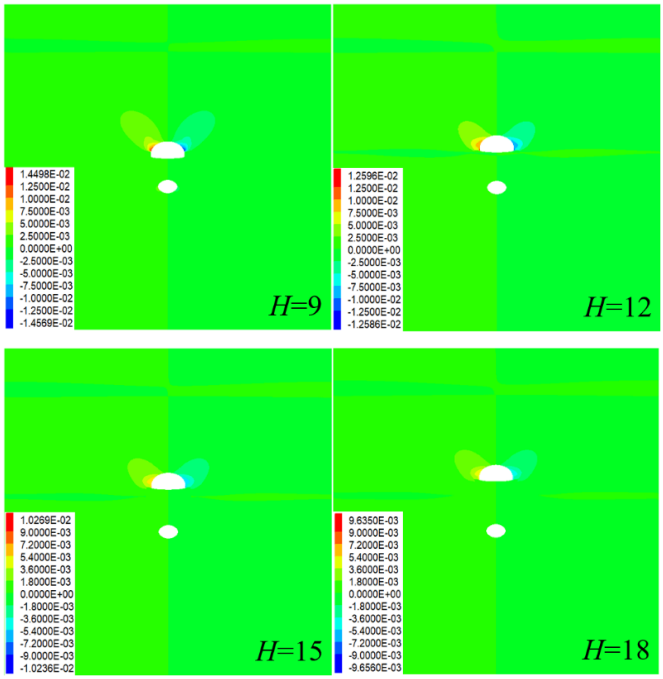

Fig. 7 Contour maps of horizontal displacement (unit: m)

(2) The contour maps of vertical displacement shows that the peak value of vertical displacement is mainly concentrated in the vault and arch bottom of the tunnel. When the tunnel is close to the goaf (H=3~H=9), the deformation of surrounding rock mass is most significantly affected by the goaf, and the deformation range and increase range are significantly larger than other working conditions. There is obvious asymmetric deformation tendency, and distortion phenomenon near the goaf. In H=12~H=18, the deformation range and deformation amplitude of surrounding rock mass are relatively gentle, and the influence of goaf can be ignored. Therefore, for the vertical displacement of tunnel surrounding rock mass, the goaf within a safe distance of 1L (i.e. 12 m) will increase the settlement degree and range of tunnel surrounding rock mass, which will bring adverse effects to tunnel construction.

(3) The contour maps of horizontal displacement shows that both sides of the tunnel by the extrusion of the surrounding rock mass are moving to the interior of the tunnel, and the deformation on both sides is roughly symmetrical and butterfly-shaped distribution. When the tunnel is closer to the goaf (H=3~H=9), the tunnel face and the goaf affect the deformation of the surrounding rock mass. The cavity of the two under the close distance further deteriorates the nature of the surrounding rock mass in this area, and the intermediate sandwich rock is looser, leading to the interconnection of the horizontal displacement zone on both sides of the elevation arch part of the tunnel and the mining area, which significantly increases the area of the horizontal displacement zone of the surrounding rock in the lower part of the tunnel. With the increase of the distance of the goaf, the influence of the underlying goaf in H=12~H=18 on the surrounding rock mass of the tunnel is weakened. However, the underlying goaf still has a great influence on the distribution of the horizontal displacement zone of the surrounding rock mass of the tunnel, and the horizontal deformation zone of the lower surrounding rock mass still extends to the cavity of the goaf. The horizontal displacement distribution of surrounding rock mass under H=15 is basically consistent with H=18.

According to the above analysis, when the distance between the goaf and the tunnel is within 1L (12 m), the underlying goaf has a significant effect on the displacement distribution of the surrounding rock mass of the tunnel. When the distance between the goaf and the tunnel is 1.25L~1.50L (15~18 m), the influence on the displacement distribution of the tunnel is weakened. When the distance between the two is greater than 1.50L (18 m), it can be considered that the goaf has no effect on the displacement distribution law of the tunnel.

To better explore the asymmetric deformation (distortion) of the tunnel structure under the influence of the goaf, the tunnel structure deformation and displacement vector (magnification factor 140) of H=6 are extracted, as shown in Figs. 8-9, respectively.

There is a mutual influence between the goaf and the tunnel, and a large vertical displacement is generated at the bottom of the tunnel and the upper part of the goaf. That is, the tunnel clearance and the goaf cavity are deformed and converged, the middle rock column on both sides of the tension, the stress environment is very bad, and the surrounding rock

mass is relatively loose. To further study the deformation of the tunnel at this location, the displacement changes of six monitoring points were extracted (Fig. 10).

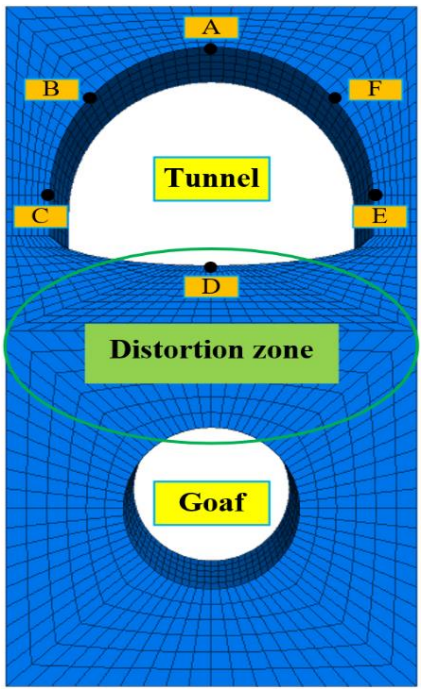

Fig. 8 Deformation diagram of tunnel structure

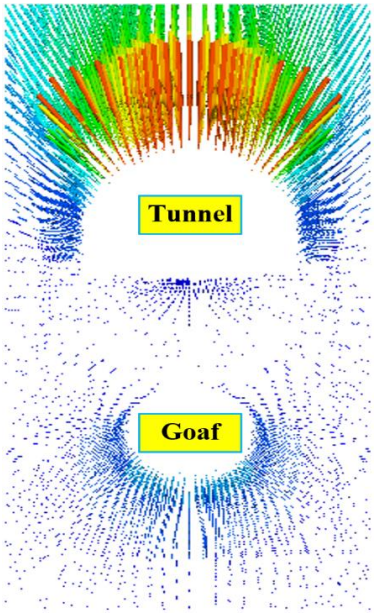

Fig. 9 Displacement vector distribution of surrounding rock

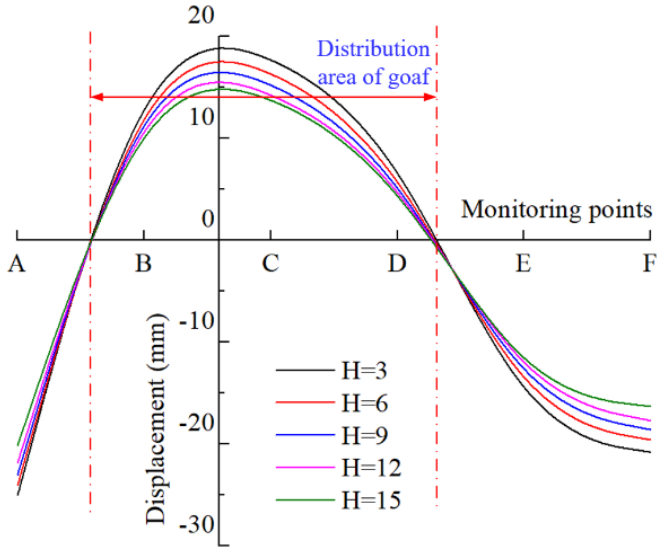

Fig. 10 Displacement curves of monitoring points

As can be seen from Fig. 10, in H=3~H=18, due to the existence of goaf, the displacement of six monitoring points has different degrees of mutation in the distribution area of goaf, which is manifested as the change of curve to negative direction. The reason is that the rock between the goaf and the tunnel tends to deform to the goaf cavity and the tunnel face respectively. The goaf cavity absorbs some of the surrounding rock deformation, which inhibits the uplift of the inverted arch part of the tunnel structure to a certain extent, showing obvious depression phenomenon. With the increase of goaf distance, the influence of goaf decreases slowly, and the curve gradually approaches the displacement curve of general tunnel.

3.2 Evolution process of stress field in surrounding rock mass

The stress variation curves of vault and two side walls of tunnel for each working condition are shown in Figs. 11-12, respectively. The negative stress value indicates that the tunnel is under pressure.

The stress curves of vault and two side walls of tunnel shows that the stress value of the tunnel vault bottom with H=3 is significantly greater than other working conditions. With the increase of safety distance, the stress value decreases rapidly, and the decrease rate of H=3~H=9 is the largest. It decreases from 9.76 MPa to 8.08 MPa at the vault of the tunnel and from 9.97 MPa to 8.52 MPa at the bottom of the tunnel, which is obviously affected by the distance. The stress value of top-to-floor in tunnel with H=12~H=18 changes very little, and the influence of the goaf on the tunnel can be considered negligible. The stress curves on the left and right sides of the tunnel are roughly symmetrically distributed. The horizontal stress on both sides of the tunnel has a great influence on the range of 15 m from the left and right sides of the tunnel center line. The farther away from the tunnel center line, the less obvious the change, and gradually approaches to the primary rock stress of surrounding rock mass.

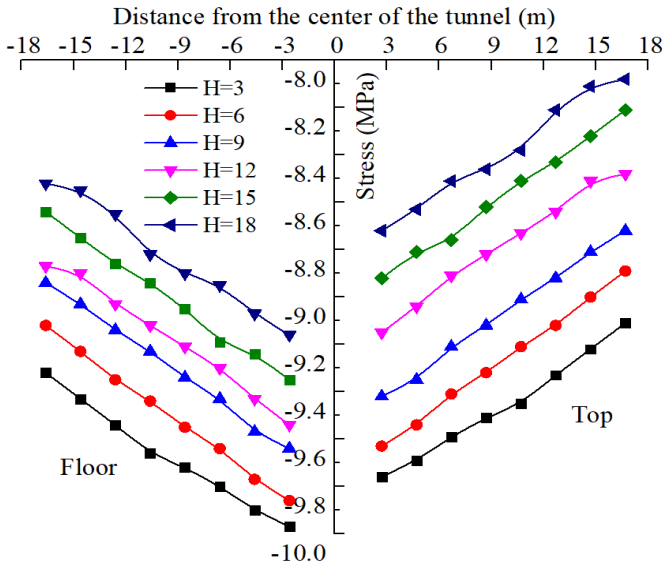

Fig. 11 Stress curves of top-to-floor in tunnel

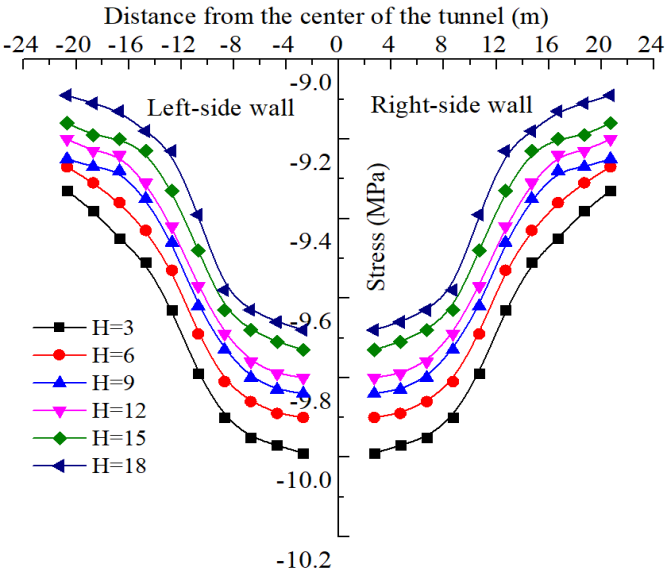

Fig. 12 Stress curves between two sides of tunnel

The contour maps of vertical and horizontal stress of surrounding rock mass in each working condition are shown in Figs. 13-14 respectively.

(1) The vertical stress contour maps shows that the stress value is negative, indicating that the tunnel is under pressure. Under the influence of blasting excavation, the stress of surrounding rock mass will be readjusted. The closer the distance from the center of the tunnel, the more obvious the stress change. With the increase of distance, the stress growth rate is relatively gentle and gradually approaches the original rock stress. Under the same stress level, the influence range of tunnel vault stress is larger than that of arch bottom, and the stress concentration occurs at the vault, and the range of stress release at the tunnel face increases. There are obvious stress concentration phenomenon from H=3~H=9, which is mainly distributed in the vault, arch bottom, and the junction of two sides and floor of tunnel. In H=12~H=18, as the distance between the goaf and the right side of tunnel increases, the stress concentration phenomenon gradually weakens.

(2) The contour maps of horizontal stress shows that the influence area of horizontal stress on the two sides of the tunnel is more than that of the roof and floor, which leads to the irregular shape of horizontal stress distribution on the two sides of the tunnel, which is approximately elliptical. With the increase of safe distance between the tunnel and the goaf, the action range of the horizontal stress contour map of surrounding rock mass increases. It shows that the selection of the best safety distance has a certain influence on the excavation of the cavern. When H=3~H=18, although the surrounding rock stress increases with the increase of safety distance, the increase is not significant.

In summary, from the perspective of the stress change level of the goaf on the tunnel structure, the goaf with a safety distance of 1L (12 m) will cause the phenomenon of stress concentration on the right side of the tunnel. It also increases the value of stress, which brings hidden danger to the safety of tunnel construction and should be paid attention to during the construction design.

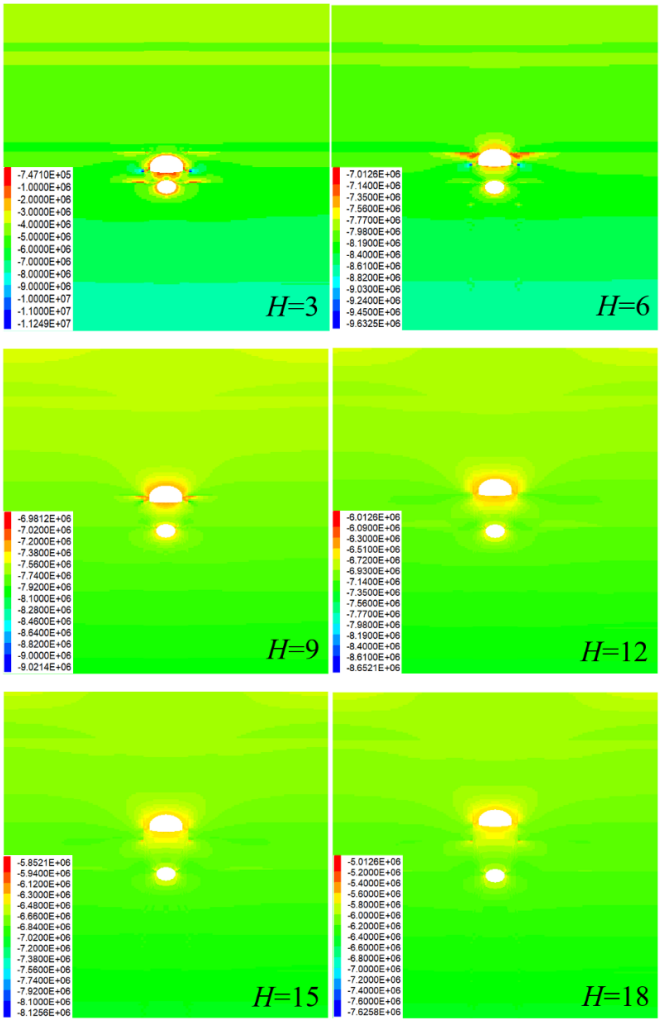

Fig. 13 Contour maps of vertical stress (unit: Pa)

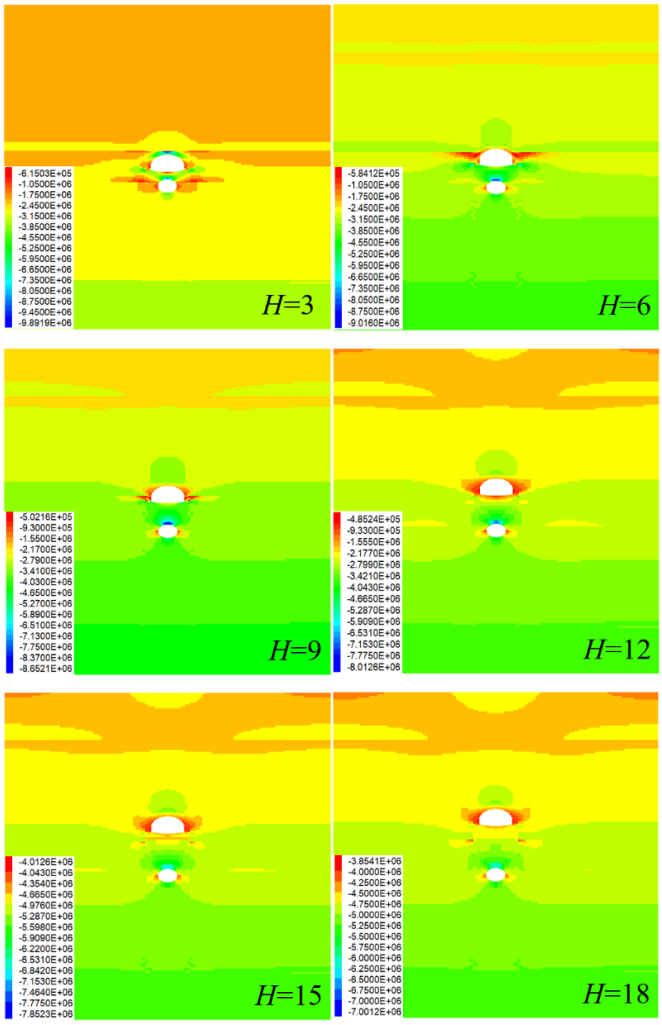

Fig. 14 Contour maps of horizontal stress (unit: Pa)

The contour maps of maximum principal stress in tunnel lining for each working condition is shown in Fig. 15. As can be seen from Fig. 15, there is an obvious stress concentration phenomenon from H=3 to H=9. The negative value of the maximum principal stress is concentrated on the left and right sides of the tunnel lining structure in the working condition where the mining area is relatively close. It means that the lining structure in this area is under severe pressure, which may lead to pressure damage of the lining. With the increase of the distance between the goaf and the right contour of the tunnel, the concentration of the maximum principal stress gradually disappears, and the maximum principal stress distribution law of H=12~H=15 is basically the same as that of H=18.

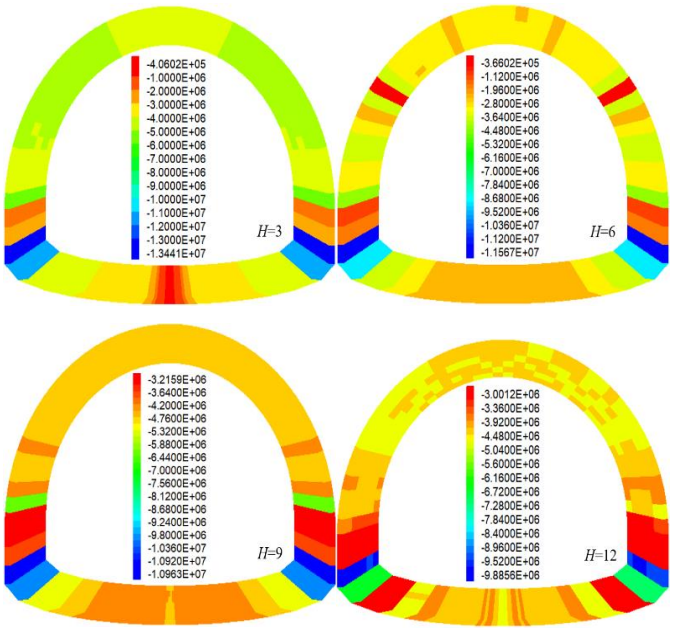

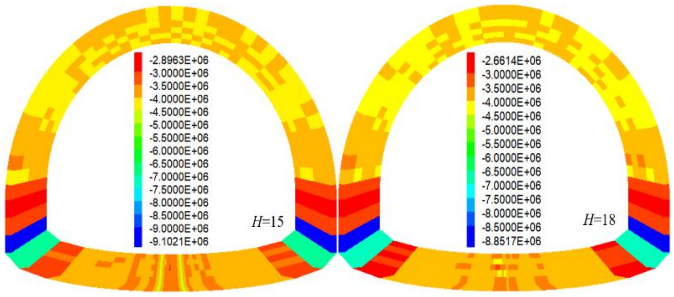

Fig. 15 Contour maps of maximum principal stress in tunnel lining (unit: Pa)

The maximum value of maximum principal stress in tunnel lining for each working condition is shown in Fig. 16.

As can be seen from Fig. 16, with the increase of goaf distance, the maximum principal stress maximum value of each working condition gradually decreases and converges to H=18. The maximum principal stress value of H=3 is obviously larger than that of other working conditions, and the maximum principal stress decreases rapidly with the increase of distance. Among them, the decrease of H=3~H=9 is the largest, from 13.44 MPa to 10.96 MPa, which is obviously affected by the distance. The maximum principal stress maximum value of H=12~H=15 has a small variation, which is basically equivalent to H=18. At this time, the influence of the goaf can be considered negligible.

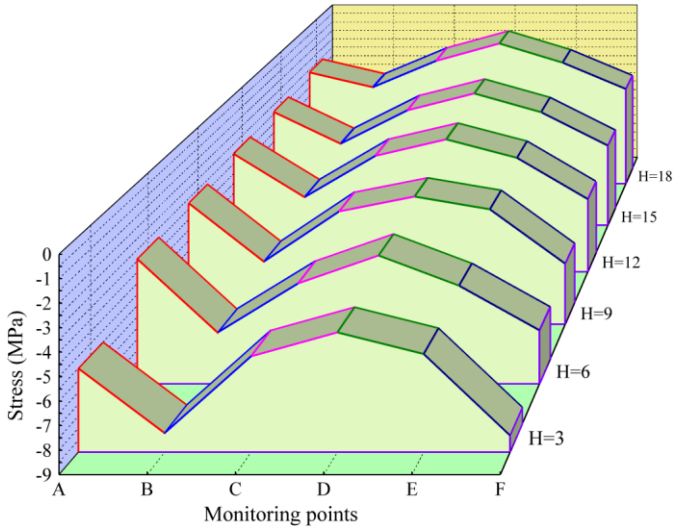

Fig. 16 Maximum value of maximum principal stress in tunnel lining

In conclusion, for the maximum principal stress of the tunnel structure, the goaf within a safe distance of 1L (12 m) will cause stress concentration on the lower side of the tunnel. At the same time, the value of the maximum principal stress is greatly increased, which brings obvious adverse effects to the tunnel structure, and attention should be paid to the construction design.

3.3 Evolution process of energy

(1) Law of energy release

The distribution of elastic strain energy density of surrounding rock mass around tunnel under different working conditions is shown in Fig. 17. The change curves of elastic strain energy density at six monitoring points in each working condition are shown in Fig. 18.

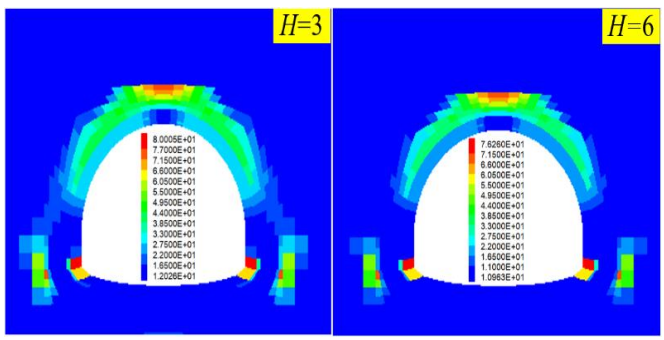

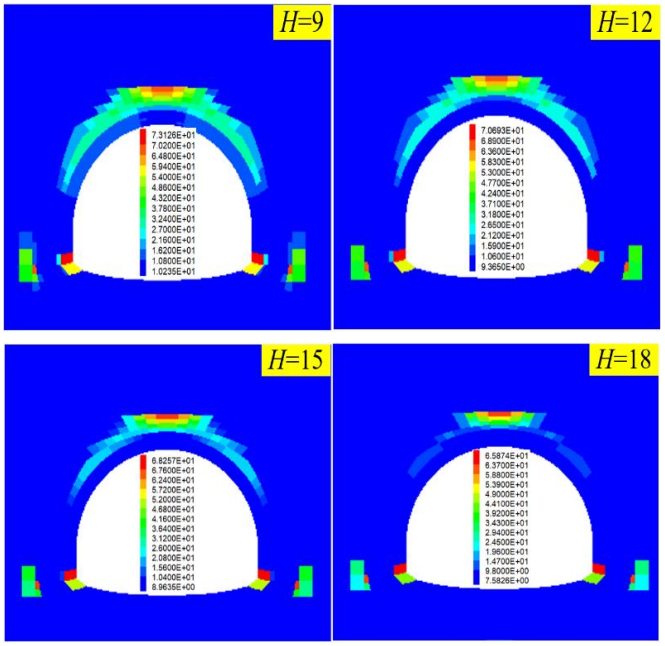

Fig. 17 Distribution of elastic strain energy density (unit: J/m3)

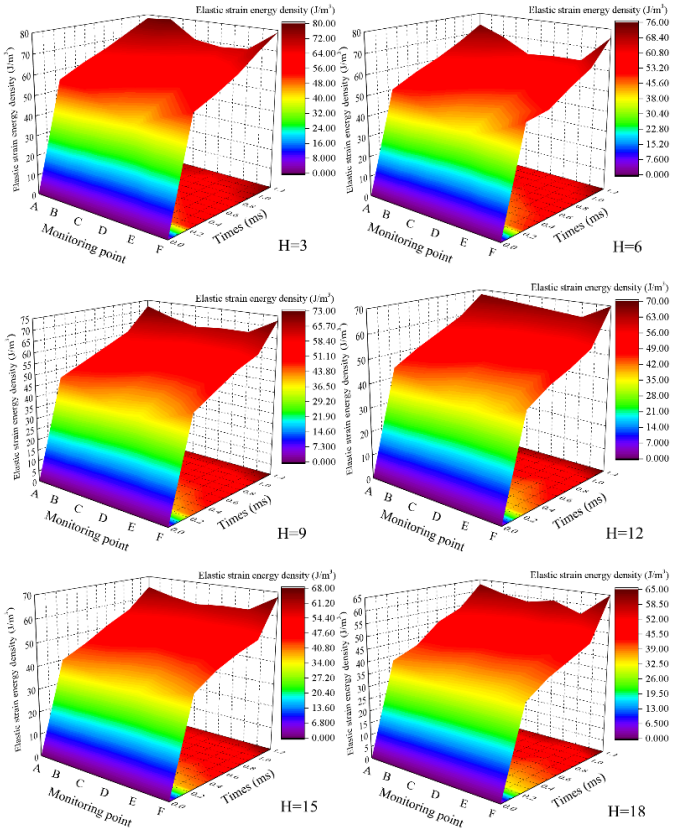

Fig. 18 Space-time distribution of elastic strain energy density

Analysis of Fig. 17~Fig. 18 shows that after the tunnel is excavated by blasting, the surrounding rock mass changed from three-way stress state to two-way stress state. Under the action of stress concentration, the surrounding rock mass of the tunnel transfers to the excavation face, and the stress field of the internal surrounding rock mass will be redistributed to form a secondary stress field. The elastic strain energy of surrounding rock mass increases with the increase of safety distance, but the increase is small. When H=3~H=9, the elastic strain energy is the largest at the vault, bottom, side wall and corner of the tunnel, resulting in more elastic energy accumulated in front of the tunnel face. If these energies are released rapidly, the rock will produce a power destabilization geohazard of bursting, loosening, peeling, ejection, throwing and other destructive phenomena. With the increase of safety distance, the elastic energy accumulated in front of the tunnel face in H=12~H=18 is less.

(2) Law of energy conversion

To explore the correlation between the energy conversion of surrounding rock mass and the change of stress ratio (the ratio of the upper limit of stress level σ_{max} to the peak stress σ_p) under blasting load. The relationship curves between the accumulated horizontal energy and

stress ratio of the tunnel at different safety distances were fitted, as shown in Fig. 19.

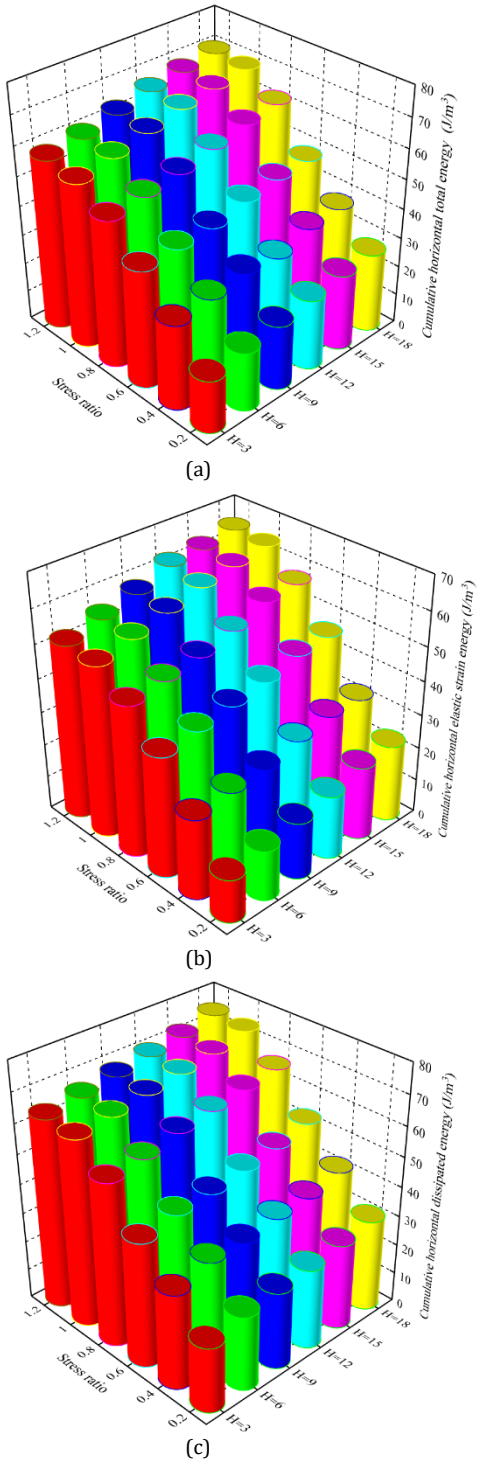

Fig. 19 Relationship between cumulative horizontal energy and stress ratio. (a) Cumulative horizontal total energy; (b) Cumulative horizontal elastic strain energy; (c) Cumulative horizontal dissipated energy

From the analysis of Fig. 19, the curves of cumulative horizontal energy and stress ratio change in roughly the same trend at different safety distances. When H=3~H=18, with the same stress level, the stress ratio decreases with the increase of safety distance, and the corresponding total cumulative level energy and elastic strain energy decrease, but the dissipation energy decreases first and then increases with the increase of safety distance. Under the same stress ratio, the cumulative total energy and elastic strain energy increase with the increase of safety distance, and the increase is higher. With the increase of stress ratio, the cumulative horizontal total energy, elastic strain energy and dissipation energy show an increasing trend.

(3) Law of energy distribution

To facilitate the visualization of the energy distribution between the tunnel and the goaf at different safety distances. The relationship curves of elastic strain energy ratio n (the ratio of cumulative horizontal elastic strain energy to cumulative horizontal total energy), dissipation energy ratio m (the ratio of cumulative horizontal dissipation energy to cumulative horizontal total energy) and dissipation energy ratio coefficient e (cumulative horizontal dissipation energy and cumulative horizontal elastic strain energy) with stress ratio are drawn, as shown in Fig. 20.

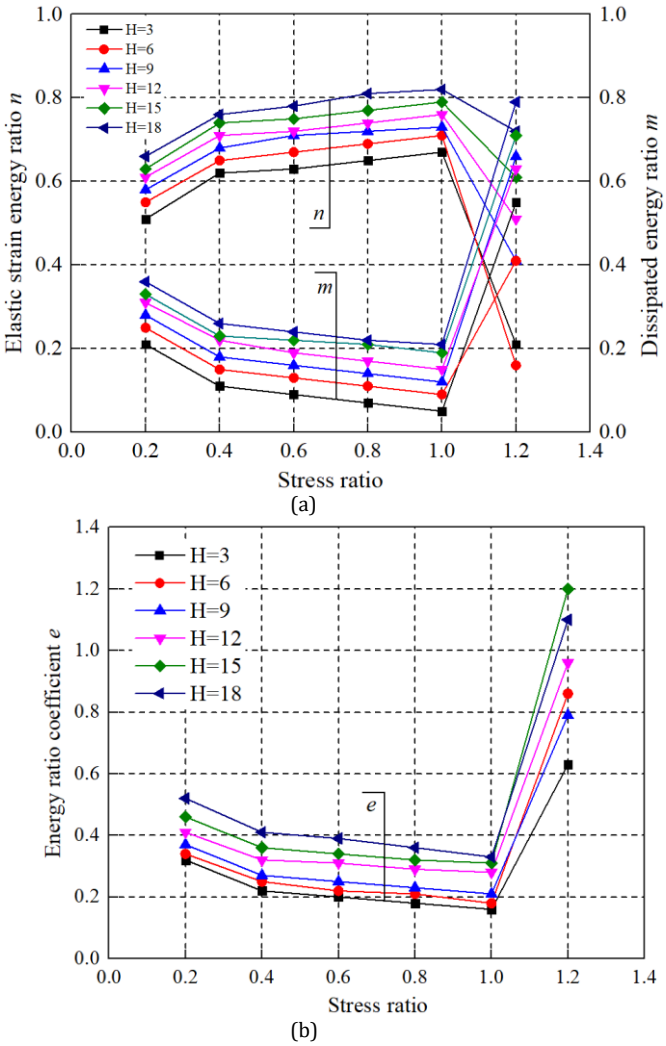

Fig. 20 Relation curves between energy ratio and energy ratio coefficient and stress ratio. (a) Energy ratio; (b) Energy ratio coefficient

As can be seen from Fig. 20, the curves of n, m and e have the same trend under different working conditions. With the increase of safety distance, n first gradually increases and then tends to stabilize until the stress level curve drops abruptly after blasting excavation, and the curve is roughly inverted U-shaped distribution. The m and e first decrease and then also stabilize, and finally the curve rises instantaneously, roughly in a U-shaped distribution. The n, m, e can not only directly reflect the energy distribution ratio of the surrounding rock mass under each stress level, but also indirectly reflect the internal damage degree and energy transformation mechanism of the surrounding rock mass in tunnel. When H=3~H=6, n and m decrease the most, and e increases the most. When H=9~H=12, n, m and e are in a relatively stable trend when the stress ratio is 0.38~0.57 and 0.61~0.82. When H=15~H=18, with the increase of safety distance, the change of n, m and e curves increases gently compared with other working conditions. In short, when H=3~H=6, the stress ratio rate at the energy weakening stage is lower and the stress ratio rate at the strengthening stage is higher.

4. Evaluation of safety and stability

In tunnel construction, the reasonable safety distance between the goaf and the tunnel determines the design factors such as tunnel alignment, buried depth and length to a certain extent. In view of the complexity of surrounding rock mass hydrogeological conditions and construction environment and the safety of later operation, it is necessary to track and monitor the on-site construction. Further adjust in time according to the feedback data to improve the safety of tunnel construction and operation. Based on the numerical test results in the previous section, the measurement points with a safe distance of 1L (i.e., 12 m) was selected for blast monitoring. The vibration velocity between the goaf and the tunnel is controlled within the scope of the national safety standard, to avoid the instability and collapse of the goaf and make the

construction smooth and safe. The arrangement of field measuring points is shown in Fig. 21, the displacement and stress monitoring curves are shown in Fig. 22, and the measured vibration velocity curves of measuring points are shown in Fig. 23.

From Fig. 22, the growth rate of surrounding rock mass deformation is faster at 0 to 15 d, and the amount of deformation is increasing. After 15 d, the deformation growth rate of surrounding rock mass is slow and gradually tends to be stable. The deformation of surrounding rock mass reaches the peak at 30 d, and the deformation of surrounding rock mass does not increase. Similarly, the growth rate of the surrounding rock mass stress is faster, and the value increases continuously from 0 to 15 d. After 15 d, the curve gradually stabilized. The surrounding rock mass stress reaches the peak at 30 d. It can be seen from Fig. 23 that the vibration velocity increases rapidly, and the velocity value increases continuously from 0 to 18 d. The vibration velocity increases slowly after 18 d, and reaches the peak at 30 d, and the vibration velocity does not increase.

Fig. 21 Site monitoring points layout

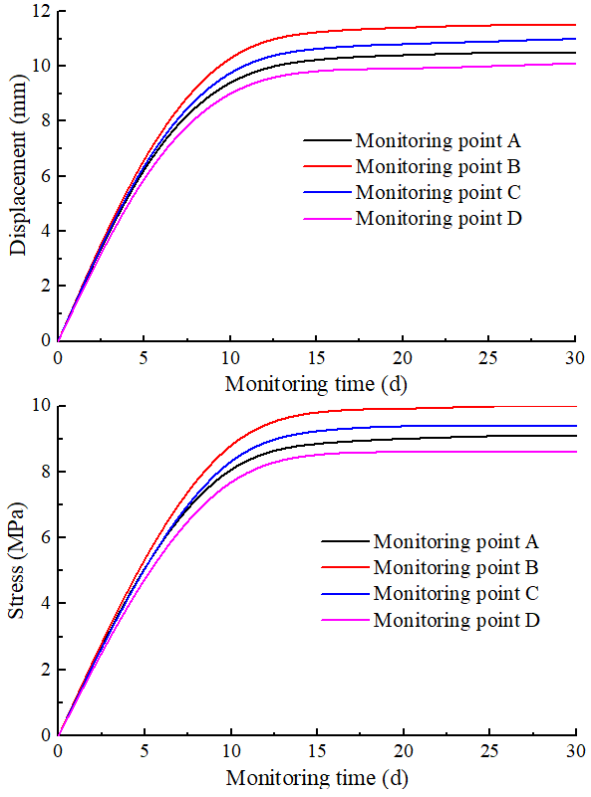

Fig. 22 Displacement and stress curve of monitoring points

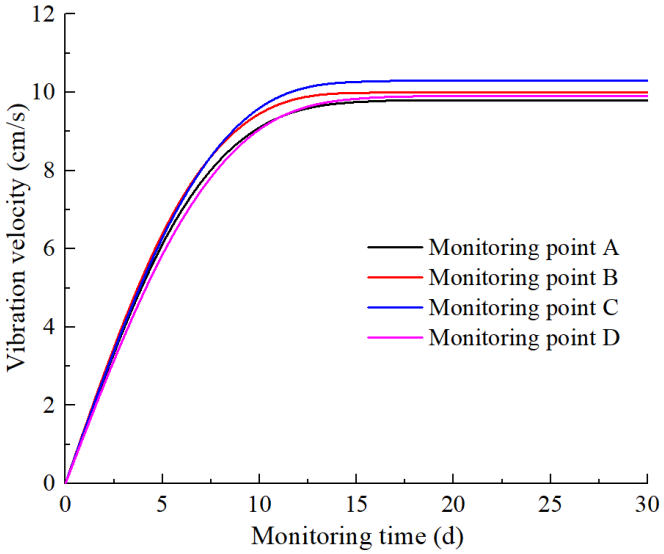

Fig. 23 Measured curves of vibration velocity at measuring points

In summary, by comparing the numerical calculation results with the field measurement results, it is found that the deformation trends of the displacement and stress curves are basically the same, and the error of the results is small. It is further verified that the numerical calculation is in good agreement with the field monitoring displacement change. From the displacement and stress monitoring curve and the measured curve of the vibration velocity of the measuring point, when the safety distance is 1L (that is, 12 m), the deformation of the surrounding rock mass around the tunnel can be slowed down, the bearing capacity of the surrounding rock mass can be improved to the maximum extent, the bearing arch of the surrounding rock mass can be formed, and the possibility of geological disasters in the surrounding rock mass can be reduced.

5. Conclusion and discussion

(1) The multi-information evolution characteristics of surrounding rock mass shows that when H=3~H=6, the influence of goaf on tunnel is very serious, and there is obvious stress concentration, which is mainly distributed in the vault, arch bottom, and the junction of two sides and bottom plate of the tunnel. When H=9~H=12, the goaf has little effect on the tunnel, but its displacement amplification effect cannot be ignored. When H=12~H=18, with the increase of the distance between the goaf and the right side of the tunnel, the stress concentration phenomenon gradually weakens. The curve between cumulative stress level energy and stress ratio can be divided into three stages: acceleration, equalization, and deceleration.

(2) The goaf is within 0.5L (6 m) from the tunnel, the goaf has a significant impact on the tunnel structure, and the tunnel structure is in the danger zone; when the goaf is 0.5L~1L (6~12 m) away from the tunnel, the influence of the goaf on the tunnel structure cannot be ignored, and the tunnel structure is in the impact zone; When the distance between the goaf and the tunnel is greater than 1L, the influence of the goaf on the tunnel structure can be neglected, and the tunnel structure is in the safe zone. The safety distance of 1L (12 m) can slow down the deformation of surrounding rock mass around the tunnel, make the surrounding rock mass form a bearing arch.

(3) The fracture catastrophe of the surrounding rock in the goaf is one of the fundamental causes of the frequent occurrence of safety accidents in the goaf of underground cavern. When the tunnel passes through the adverse geological section of the goaf, the reasonable determination of the safety distance between the tunnel and the goaf is the most important issue concerning the stability of the tunnel and the safety of construction and operation. The safe distance between the tunnel and the goaf is not only a safety problem, but also an important economic factor. How to consider the stability and safety of the tunnel, the study of reasonable determination of the safety distance between the tunnel and the safe has a very important engineering significance.

In the future research work, the following aspects should be strengthened: The stability evaluation of goaf is closely related to the existence of groundwater. In particular, the loss of groundwater in the goaf has a huge impact on stability. To further study the impact of groundwater changes on the stability of the extraction zone and to seek the best management options. Combined with more mechanical models and analysis methods, the failure mechanism of the surface and roof overburden of the underlying goaf is studied.

Acknowledgments

This study was financially supported by the National Natural Science Foundation of China (Grant No.: 51474097, U1810203).

Disclosure statement

The authors declare that they have no conflicts of interest.

References

Chu WJ (2020) Research on the geological line selection of Baotou-Yinchuan high-speed railway in Gander Mountain area. Journal of Railway Engineering Society 37(06): 5-9.

Cui LY (2019) Stability analysis on surrounding rock of deep buried tunnel passing through complex goaf. Chinese Journal of Underground Space and Engineering 15(S2): 710-716.

Fu X, Liu X, Wu QX, Chang T, Wang YF, Sha HH (2024) Experimental simulation study on gas flow field in combined goaf during the transition period of coal pillar-free working face relocation. Physics of Fluids 36(1): 016605.

He WX (2017) Study on vibration characteristics of surrounding rock induced by tunnel excavation blasting. Wuhan: Wuhan University.

Islavath SR, Katkuri S, Deb D, Kumar H, Prasad M (2022) Negotiating an inclined normal fault in a longwall panel: A case study. International Journal of Coal Geology 251: 103935.

Lei S, Fang Y, Liu J, Huang L (2019) Research of construction ventilation optimization for Huayingshan tunnel on Nanchong-Dazu-Liangping expressway. Modern Tunnelling Technology 56(02): 194-200.

Liu Q, Lin BQ, Zhou Y, Yanjun Li YJ (2023) Constitutive relation and particle size distribution model of rock fragments in the goaf. Environmental Science and Pollution Research https://doi.org/10.1007/s11356-022-25038-6

Peng WB (2020) FLAC3D practical tutorial. Beijing: China Machine Press.

Ram S, Singh AK, Kumar R, Kumar A, Kumar N, Waclawik P, Gautam A, Raja M (2021) Design of rock bolt-based goaf edge support for conventional depillaring with stowing. Arabian Journal of Geosciences 14(21):1-13.

Vinay LS, Bhattacharjee RM, Ghosh N, Budi G, Kumar JV, Kumar S (2022) Numerical study of stability of coal pillars under the influence of line of extraction. Geomatics, Natural Hazards and Risk 1556-1570

Wang B, Lv Y, Liu C (2024) Research on fire early warning index system of coal mine goaf based on multi-parameter fusion. Scientific Reports 14: 485.

Wang HL (2020) Study on safety stability evaluation and treatment measures of highway tunnel structures in underground goaf. Highway 65(02): 308-315.

Wang YH, Si GY, Xiang ZZ, Oh J, Belle B, Webb D (2022) A theoretical goaf resistance model based on gas production analysis in goaf gas drainage. International Journal of Coal Geology 264: 104140.

Xu ZC, Xu W, Zhu ZH, Zhao JY (2023) Research on monitoring and stability evaluation of ground subsidence in gypsum mine goaf. Frontiers in Environmental Science 10: 1097874.

Zhao B, Zhang HL, Wang Y, Zhou YT, Zhang JX (2023) Mechanical Behavior of Gas-Transmission Pipeline in a Goaf. Processes 11(4): 1022.

Zhang C, Zhao YX, Bai QS (2021) 3D DEM method for compaction and breakage characteristics simulation of broken rock mass in goaf. Acta Geotechnica 17: 2765-2781.

Zhang QL, Wang CH, Han L, Hao JW, Qiao L, Chen SF (2023) Study on Stability analysis and treatment of underground goaf in metal mine. Mining, Metallurgy & Exploration 40: 1973-1985.

Zhang ZP, He YY, Liang JG, Ren JJ, Zhao J, Fu GF (2019) Mechanical property analysis of constructing tunnel underlying inclined coal mined-out area. Tunnel Construction 39(S2): 8-16.

Zheng YN, Li QZ, Zhang GY, Zhao Y, Zhu PF, Ma X, Li XW (2021) Study on the coupling evolution of air and temperature field in coal mine goafs based on the similarity simulation experiments. Fuel 283: 118905.

Zhou H, Yang FJ, Zhang CQ, Lu JJ (2015) Methods for numerical simulation and evaluation of rock burst and rock burst. Beijing: Science Press.